

On the Constrained Walking of the NAO Humanoid Robot

Jesus E. Fierro¹, J. Alfonso Pamanes^{1(✉)}, Hector A. Moreno²,
and Victor Nunez³

¹ Instituto Tecnológico de la Laguna, Torreón, Mexico
japamanesg@correo.itlalaguna.edu.mx

² Universidad Autónoma de Coahuila, Monclova, Mexico

³ Universidad Politécnica de Sinaloa, Mazatlán, Mexico

Abstract. The legs of the NAO humanoid robot have only 11 DOF; consequently, the motion of the pelvis and the free foot cannot be entirely specified in order to fully controlling the zero moment point (ZMP) in the contact area of the support foot. Thus, constraints on motion of both the pelvis and free foot must be appropriately taken into account in the motion planning process in order to specify suitable stable gaits. Specifically, the take-off and landing of the free foot have to be achieved in such a way that undesirable forces in the contact point with the floor be avoided. In this paper, a procedure is proposed to planning suitable walks in such a way that contact between the foot and the floor produces a stable behavior of the robot. To the knowledge of the authors, this problem has not be previously studied in the literature. The proposed method is applied in a study case to show its efficacy to get a stable gait.

1 Introduction

The research on humanoid robots has been expanding since the creation of the WABOT-1 in 1973 in Waseda University [1] and then moving forward to the year 2000 with the creation of the ASIMO robot by Honda [2]. Further advances led us to the All-new ASIMO [3] in 2011 and comparable humanoid robots like the HRP-4C [4] and the Robonaut 2 [5]. Then, a few years later arrives the humanoid Nao robot [6], in which this paper takes a closer look.

In regards of motion planning for biped robots there has been several approaches, like footstep planning [7,8] and walking patterns. The study in [9] is based on walking of humans and the efficiency that brings emulating the extended knee walk in our natural pattern. Other way of approaching the walking control problem is by generating trajectories based on the inverted pendulum model [10,11] or by using fuzzy logic systems as seen in [12] which brings a faster response for the online walking mode. Previous particular works on the Nao robot were presented in [13,14] where the motion planning is based on the inverse pendulum approach. On the other hand, a gait planning focused on energy efficiency was proposed in [15]. A similar kinematic model of the robot was applied in [16]. The methods proposed in all these works give interesting schemes of walking for

that humanoid. However, constraints on motion of the pelvis and the free foot of the robot were not explicitly taken into account and therefore the ZMP cannot be fully controlled; as consequence, a stable walking could not be guaranteed by applying such approaches. In this paper, a procedure is proposed to define a suitable walking in such a way that full contact between the foot and the floor be achieved. As result, a feasible stable behavior of the robot could be obtained for constrained motions of the pelvis and the free foot during the walking. A section is included to present the constraints that exist in motion of the pelvis and the free foot. The proposed method is finally applied in a study case that show its efficacy in getting a suitable walking.

2 Humanoid Robot NAO

Made by the Aldebaran Robotics Company, the Nao is a programmable humanoid robot with 25 DOF: five for each arm and one for each hand, two for the head, and eleven for the legs. It has 0.57 m of height and 4.5 kg of weight. The robot is shown in Fig. 1 and the kinematic scheme corresponding to the legs is appreciated in Fig. 2. Each leg has six rotational joints, but the motion of the joints attached to the pelvis are constrained in such a way that one actuator produces symmetrical rotations on them, as shown in Fig. 3.

To describe the kinematic chain of the Nao, we apply the modified Denavit-Hartenberg notation [17]. One orthonormal reference frame is attached to each link. The links are numbered from 0 to 12 starting with the fixed link (support



Fig. 1. The Nao humanoid robot from the Aldebaran Company.

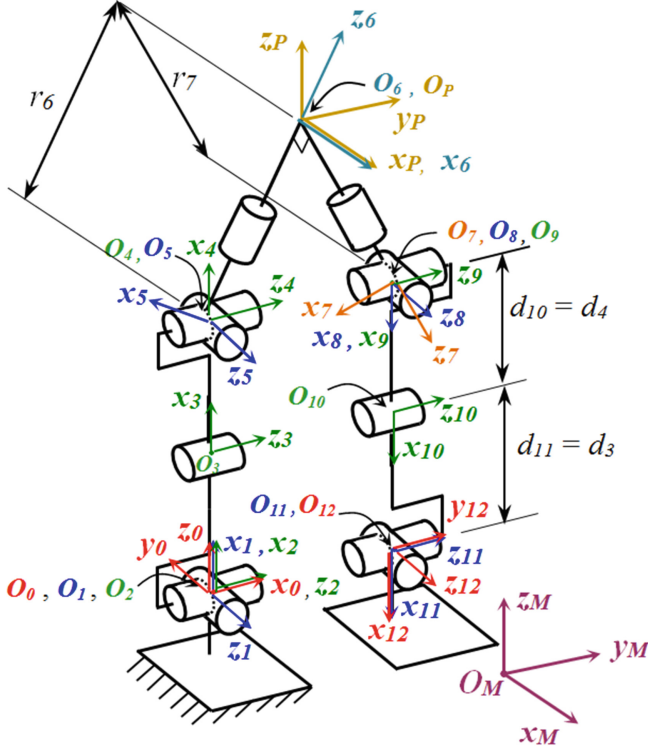


Fig. 2. Kinematic scheme of legs of the Nao robot

foot) and ending on the moving foot (free foot), as shown in Fig. 2. In this figure, we can also appreciate the orthonormal frame $x_M - y_M - z_M$ attached to the floor (*world frame*).

For the kinematic analysis of the walking pattern, we establish two sets of reference frames in the same kinematic chain: one for the fixed right foot (*frf*), and the corresponding one of the fixed left foot (*flf*). The kinematic chain showed in Fig. 2 is that one corresponding to *frf*. In both cases *frf* and *flf*, the numeration of frames begins with zero, assigned to the fixed foot. The modified Denavit-Hartenberg (MDH) parameters of the kinematic chain for the legs are given in Table 1. These parameters are the same for both chains *frf* and *flf*. The values for the non-null distances in Table 1 are $d_3 = d_{11} = 0.103 \text{ m}$, $d_4 = d_{10} = 0.10 \text{ m}$ and $r_6 = r_7 = 0.0712 \text{ m}$.

In the power transmission scheme of Fig. 3 we can appreciate how a single motor provides motions to joints 6 and 7 attached to the pelvis of the kinematic chain. Thus, the following constrain is imposed by the power transmission:

$$\theta_7 = \theta_6 \quad (1)$$

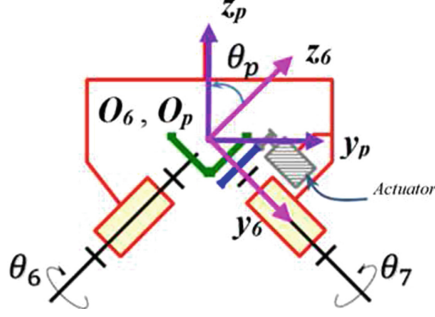


Fig. 3. Scheme of the power transmission to joints attached to the pelvis

Table 1. Modified Denavit-Hartenberg parameters for the legs of the Nao

	α	d	θ	r
1	90°	0	θ_1	0
2	90°	0	θ_2	0
3	0°	d_3	θ_3	0
4	0°	d_4	θ_4	0
5	-90°	0	θ_5	0
6	90°	0	θ_6	r_6
7	-90°	0	θ_7	r_7
8	90°	0	θ_8	0
9	-90°	0	θ_9	0
10	0°	d_{10}	θ_{10}	0
11	0°	d_{11}	θ_{11}	0
12	90°	0	θ_{12}	0

This equation holds while the robot is moving and, evidently, restrain the mobility of the kinematic chain. One orthonormal reference frame (frame $x_p - y_p - z_p$) attached to the pelvis is shown in Fig. 3. This frame is rotated by a fixed angle θ_p with respect to the x_6 axis of frame 6. Note that $\theta_p = 45^\circ$ for *frf* and $\theta_p = -45^\circ$ for *flf*.

3 Elemental Walking Pattern

A general walking pattern is defined by specifying the poses (position and orientation) of the frames attached to the pelvis (frame $x_p - y_p - z_p$, Fig. 2) and the free foot (frame $x_{12} - y_{12} - z_{12}$, Fig. 2) with respect to the world frame as functions of time. In previous works [18] we have used closed cycloidal functions to define both motions. However, as established in Sect. 1, other approaches have

been applied to specify the gait of humanoid robots. A particular case of walking for a humanoid is obtained when the frame $x_p - y_p - z_p$ remains parallel to the frame $x_m - y_m - z_m$ and the sole of the free foot remains parallel to the plane $x_M - y_M$ of the world's frame during the walk. This kind of walking will be termed *elemental walking* in this paper. In such a walking, the displacement of the torso is only translational while the motion of the free foot is general but constrained to have rotations only about z_m . The desired orientation of the pelvis and the free foot will be specified with respect to the world's frame by using the Bryant angles λ, μ, ν , which corresponds respectively to successive rotations about the axes x, y, z attached to the corresponding link beginning with this frame matched with the world's frame. Thus, in elemental walking the three Bryant angles of the pelvis are nulls, and therefore, the rotation matrix of the pelvis with respect to the world's frame is:

$${}^M_p R^* = \begin{bmatrix} t_{11} & t_{12} & t_{13} \\ t_{21} & t_{22} & t_{23} \\ t_{31} & t_{32} & t_{33} \end{bmatrix} = \begin{bmatrix} 1 & 0 & 0 \\ 0 & 1 & 0 \\ 0 & 0 & 1 \end{bmatrix} \quad (2)$$

For rotation of the free foot in elemental walking, we only specify the orientation of the vector x_{12} of the foot frame. To hold the conditions of an elemental walking, such a vector must be normal to the floor surface (plane $x_M - y_M$). Hence, the rotation matrix for the free foot with respect to the world's frame is:

$${}^M_p R^* = \begin{bmatrix} m_{11} & m_{12} & m_{13} \\ m_{21} & m_{22} & m_{23} \\ m_{31} & m_{32} & m_{33} \end{bmatrix} = \begin{bmatrix} 0 & m_{12} & m_{13} \\ 0 & m_{22} & m_{23} \\ -1 & 0 & 0 \end{bmatrix} \quad (3)$$

The terms m_{12} , m_{13} , m_{22} and m_{23} in this matrix are defined by the values specified for λ , μ and ν . In a previous analysis of the elemental walking [19] it was proved that for a specified pose of the pelvis and a specified position of the free foot, the terms m_{12} , m_{13} , m_{22} and m_{23} must hold the following equations:

$$-c_7 s_8 m_{13} + (c_P c_8 + s_P s_7 s_8) m_{23} = 0 \quad (4)$$

$$\begin{aligned} & [c_7^2 c_8^2 + s_7^2] m_{13}^2 + 2[c_7 c_8 (c_P s_8 - s_P s_7 c_8) + s_7 c_7 s_P] m_{13} m_{23} \\ & + [(c_P s_8 - s_P s_7 c_8)^2 + s_P^2 c_7^2] m_{23}^2 = 1 \end{aligned} \quad (5)$$

where $s_i \equiv \sin \theta_i$, $c_i \equiv \cos \theta_i$ ($i = 7, 8$), $s_p \equiv \sin \theta_p$ and $c_p \equiv \cos \theta_p$. The angles θ_7 and θ_8 are the joint variables corresponding to joints 7 and 8, respectively, of the kinematic chain of Fig. 2.

For an elemental walking the Bryant angles of the free foot are constrained in such a way that m_{12} , m_{13} , m_{22} and m_{23} hold Eqs. (4) and (5). These equations are defined in [19] as the *conditions for an elemental walking*. During a walk, these conditions are accomplished if the path of the point O_p of the pelvis remains on the sagittal plane of the robot, and the point O_{12} of the free foot remains on a plane parallel to the sagittal plane. Otherwise, the sole of the free foot will not be parallel to the plane of the floor and a stable contact of the foot with the floor could not be achieved.

4 General Walking

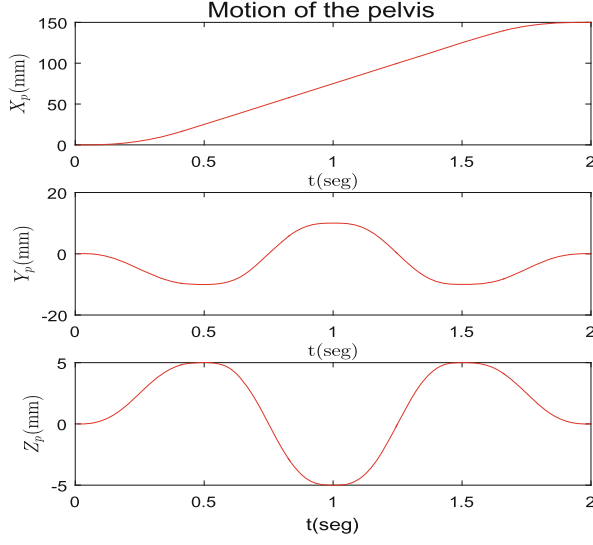
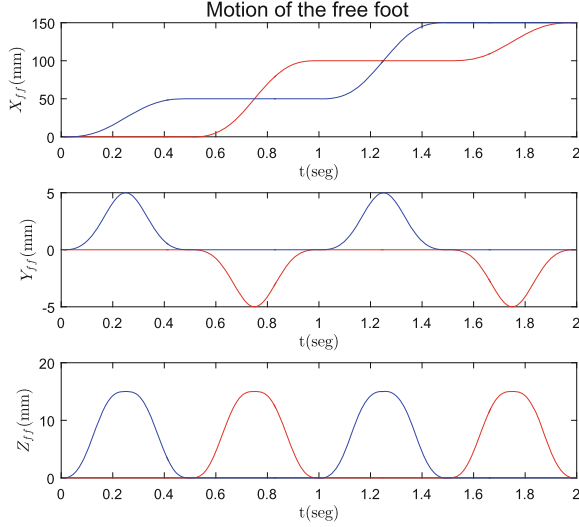
As shown in the precedent Section, for an elemental walking of the Nao robot it is possible to obtain poses of the support foot such that a full contact of the sole with the floor is achieved. Nevertheless, under elemental walking, the point O_p of the pelvis is constrained to remain on the sagittal plane. This condition generally do not allow keeping the ZMP in the support surface of the robot during the single support phase. Thus, in order to fully controlling the position of the ZMP, a component of motion of the point O_p must be on the frontal plane. Such a component, nevertheless, avoids the elemental walking; consequently, the conditions for elemental walking must be disregarded if we want improve the position of the ZMP in the sole of the support foot. We propose to retain the full contact condition of the support foot (Eq. 3), but admitting rotations and displacements of the pelvis on the frontal plane. Therefore, the positions and orientations of the free foot and the positions of the pelvis will be fully specified. The rotations of the pelvis will be admitted in order to improve the mobility of the free leg to suitably controlling the ZMP. To specify the orientation of the free foot we apply the Bryant angles $\lambda_{12}, \mu_{12}, \nu_{12}$ that define the orientation of frame 12 with respect to the world's frame. The Bryant angles λ_p, μ_p and ν_p of the orientation of the pelvis are determined by the joint variables θ_4, θ_5 and θ_6 of the support leg. Because of λ_p, μ_p and ν_p are not specified, then θ_4, θ_5 and θ_6 will be considered as the independent variables of an optimization method. Indeed, to solve the inverse kinematic problem by using only 11 DOF for the partially specified motion of the robot we propose a numerical procedure based on a non-linear optimization method. The phases of this procedure are:

1. To specify the Cartesian coordinates x_p, y_p, z_p of the point O_p in pelvis, and $x_{O12}, y_{O12}, z_{O12}$ of the point O_{12} of frame attached to the free foot, and the Bryant angles $\lambda_{12}, \mu_{12}, \nu_{12}$ that define the orientation of frame 12 with respect to the world's frame.
2. To propose initial values of the joint variables θ_4, θ_5 and θ_6 .
3. By starting with the proposed initial values of θ_4, θ_5 and θ_6 , minimize the following objective function:

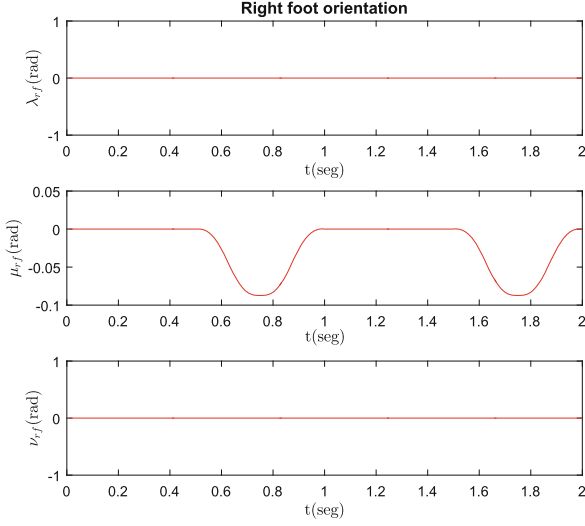
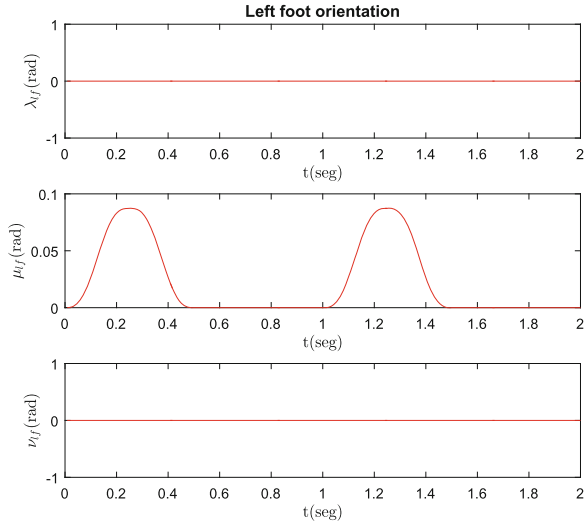
$$f = (\theta_7^* - \theta_7)^2 \quad (6)$$

The joint variable θ_7^* in Eq. (6) is the value of the 7th joint variable of the free leg that ideally should have the Nao robot considered as one of 12 DOF and, therefore, without the constraint of Eq. (1). On the other hand, θ_7 is the current value of that joint variable in the optimization process. Such a value is obtained by considering the real architecture of 11 DOF and by taking into account the constraint of Eq. (1).

Note that by following the proposed procedure at each path point, when the convergence be attained the objective function must be zero and the specified pose of the free foot will be obtained. In this case, the specified pose of the free foot and the specified position of the pelvis are fully accomplished.

**Fig. 4.** Motion of the pelvis**Fig. 5.** Position of feet

The orientation of the pelvis will be such that cooperate as much as possible with the free leg in order to get the desired pose of the free foot. At each iteration of the optimization process, for any time during the walking, by using the current set of values of the independent variables θ_4, θ_5 and θ_6 the other joint variables of the robot are computed by applying the inverse kinematic model

**Fig. 6.** Orientation right foot**Fig. 7.** Orientation left foot

proposed in [18]. At this step of the procedure, both variables θ_7^* and θ_7 are computed; the former by considering the robot as one of 12 DOF, and the second by considering the robot as one of 11 DOF. To minimize the function (6), we use the *fminunc* function in Matlab[©] software (Figs. 6 and 7).

5 Case Study

We apply in this Section the proposed approach for a general walk of the Nao robot in which the desired motions of the pelvis and the free foot are specified by using the pattern previously proposed in [20]. Only the rotational motion of the pelvis is synthesized as result of our approach. The functions defining the applied walking pattern are presented in Appendix A, and the equations of the inverse kinematic model are given in the Appendix B. The period of the specified walking is 0.5 seg for one step. The walking consists of 4 steps; the first step corresponds to the beginning phase and the last step is for the ending phase. The steps two and three are in the cruiser phase with constant velocity. The other parameters of the walking pattern are given in Table 2. In Figs. 4 and 7 are observed the curves of the desired motion of the pelvis and the free foot corresponding to the specified walking pattern, and a simulation for the desired motion of the pelvis and feet obtained in Matlab[®] is appreciated in Fig. 8. On the other hand, as result of application of our approach the joint trajectories of the Nao were obtained. A sample of postures of the robot during the walking obtained by simulation can be appreciated in the Fig. 9.

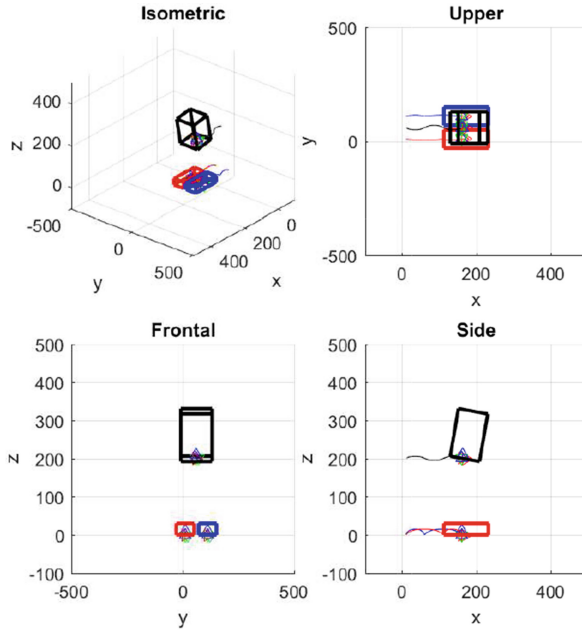


Fig. 8. Simulation of the proposed motion for the pelvis and the free foot.

Table 2. Values proposed for the parameters of the walking pattern

Parameters	Values
ns	4 steps
T_1	0.5 s
T_2	0.5 s
T_3	0.5 s
T_4	0.5 s
T	2 s
x_{pini}	10 mm
y_{pini}	60 mm
z_{pini}	200.7 mm
δx_p	150 mm
δy_p	-10 mm
δz_p	5 mm
λ_{pini}	0°
μ_{pini}	10°
ν_{pini}	0°
Parameters	Values
$\delta \lambda_p$	-5°
$\delta \mu_p$	0°
$\delta \nu_p$	0°
x_{fini}	10 mm
y_{fini}	10 mm
z_{fini}	150 mm
δx_f	150 mm
δy_f	5 mm
δz_f	15 mm
λ_{fini}	0°
μ_{fini}	0°
ν_{fini}	0°
$\delta \lambda_f$	0°
$\delta \mu_f$	-5°
$\delta \nu_f$	0°

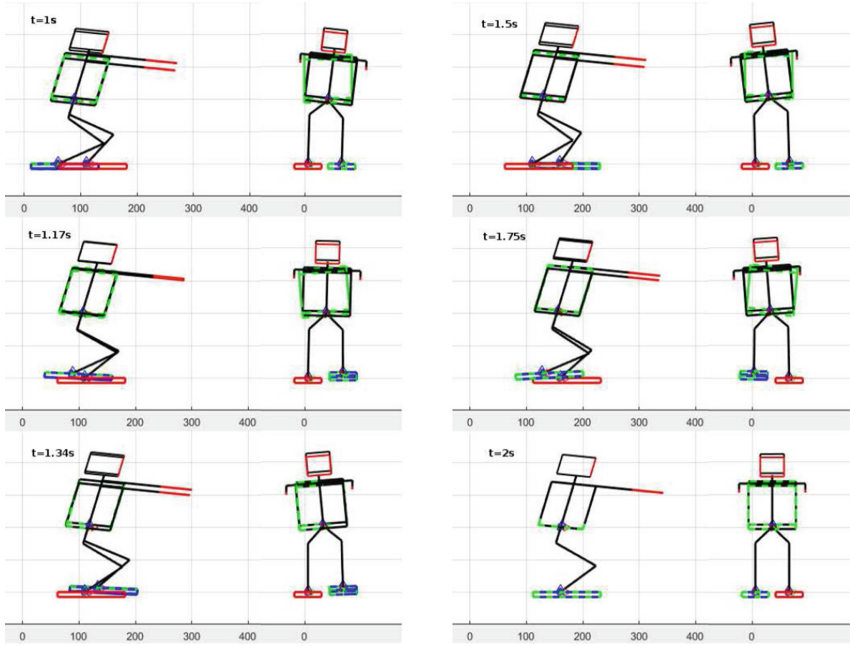


Fig. 9. Walking simulation

6 Conclusion

A study was developed in this paper for walking planning of the Nao robot. A method is proposed in order to find a suitable gait for the humanoid. The obtained results show that continuous motion of the robot and stable contact of the free foot with the floor at each step are achieved by using our approach. This one allows to solve the inverse kinematic problem of the legs with 11 DOF of the Nao humanoid for a suitable walking pattern of the robot. The motion of the free foot is fully specified while only the path of one point of the pelvis is stipulated. In this way, the translational motion of the pelvis would allow improve the control of the ZMP during the single support phase, while the rotational motion of the pelvis is synthesized in such a way that the full control for poses of the free foot is gotten. To the knowledge of the authors there are not previous studies in the literature about this subject. In future works about the gait of the Nao robot, a formulation for an optimization problem will be proposed in order to obtain the parameters of the walking pattern that improve as much as possible the behavior of the ZMP during the walking.

Acknowledgements. This work was supported by the DGTN (General Direction of the National Institute of Technology) of the Ministry of Public Education of Mexico, and the CONACyT (National Council of Research and Technology) of Mexico.

Appendix A Walking Pattern Based in Cycloidal Motions

Motion of the pelvis

It is assumed that the robot is walking in a straight line in the direction of x_M , this walking pattern is divided in three phases: *Phase 1* or initial; *Phase 2* of constant velocity or cruiser; and *Phase 3* of the stopping. During *Phase 1*, the pelvis accelerates from rest following a startup semi-cycloidal motion until it reaches just below the cruiser velocity (V_{max}); this phase happens during the first step of the walking simulation, and its period is equal to T_1 ; it is assumed that the initial posture of the robot has the feet together. A step in the constant velocity phase is done in a T_2 period. Finally, on *Phase 3* the magnitude of the velocity of the pelvis slows down following a detention semi-cycloidal motion in a T_3 period, which corresponds to a single step, arriving at a detention with both feet together. In each step on each of the three phases mentioned there is a double support phase (*DSP*) and a single support phase (*SSP*). Thus $T_i = T_{Si} + T_{Di}$ where T_i is the total period in a single step in the phase i ($i = 1, 2, 3$), T_{Si} is the period corresponding to the *SSP* in the phase i , and T_{Di} is the period of the *DSP* in phase i . Taking into account the aforementioned, the robot would be in phase 1 if $0 \leq t \leq T_1$; and in phase 2 if $T_1 < t \leq (T_1 + n_p T_2)$; and in phase 3 if $(T_1 + n_p T_2) < t \leq T_T$, where n_p is the number of steps on constant velocity, t is the actual time (elapsed time since de startup) and T_T its the total time of the walking simulation ($T_T = T_1 + n_p T_2 + T_3$). The proposed movement motions for the pelvis are shown in Eqs. (A.1)–(A.7)

$$x_p(t) = \begin{cases} \frac{S_x}{2} \left(\frac{t}{T_1} - \frac{1}{\pi} \sin\left(\frac{\pi t}{T_1}\right) \right) & , 0 \leq t \leq T_1 \\ S_x \left(j - \frac{1}{2} + \frac{t'}{T_2} \right) & , 0 \leq t' \leq T_2 \\ nS_x + \frac{S_x}{2} \left(1 + \frac{t''}{T_3} + \frac{1}{\pi} \sin\left(\frac{\pi t''}{T_3}\right) \right) & , 0 \leq t'' \leq T_3 \end{cases} \quad (\text{A.1})$$

where $j = 1, \dots, n_p$

$$y_p(t) = \begin{cases} y_{po} - \delta_{yp} \left(\frac{t}{T_1} - \frac{1}{2\pi} \sin\left(\frac{2t\pi}{T_1}\right) \right) & , 0 \leq t \leq T_1 \\ y_{co} + 2\delta_{yp} \left(\frac{t'}{T_2} - \frac{1}{4\pi} \sin\left(\frac{4t'\pi}{T_2}\right) \right) & , 0 \leq t' \leq \frac{T_2}{2} \\ y_{co} + 2\delta_{yp} \left(1 - \frac{t'}{T_2} + \frac{1}{4\pi} \sin\left(\frac{4t'\pi}{T_2}\right) \right) & , \frac{T_2}{2} \leq t' \leq T_2 \\ y_{co} + \delta_{yp} \left(\frac{t''}{T_3} - \frac{1}{2\pi} \sin\left(\frac{2t''\pi}{T_3}\right) \right) & , 0 \leq t'' \leq T_3 \end{cases} \quad (\text{A.2})$$

$$z_p(t) = \begin{cases} z_{po} + \epsilon_p \delta_{zp} \left(\frac{t}{T_1} - \frac{1}{2\pi} \sin\left(\frac{2t\pi}{T_1}\right) \right) & , 0 \leq t \leq T_1 \\ z_{po} + 2\epsilon_p \delta_{zp} \left(\frac{t'}{T_2} - \frac{1}{2\pi} \sin\left(\frac{2t'\pi}{T_2}\right) \right) & , 0 \leq t' \leq T_2 \\ z_{po} + \epsilon_p \delta_{zp} \left(\frac{t''}{T_3} - \frac{1}{2\pi} \sin\left(\frac{2t''\pi}{T_3}\right) \right) & , 0 \leq t'' \leq T_3 \end{cases} \quad (\text{A.3})$$

$$\lambda_p(t) = \begin{cases} \lambda_{po} - \epsilon_p \delta \lambda_p \left(\frac{t}{T_1} - \frac{1}{2\pi} \sin\left(\frac{2t\pi}{T_1}\right) \right) & , 0 \leq t \leq T_1 \\ \lambda_{po} + \epsilon_p \delta \lambda_p \left(1 - 2 \left(\frac{t'}{T_2} - \frac{1}{2\pi} \sin\left(\frac{2t'\pi}{T_2}\right) \right) \right) & , 0 \leq t' \leq T_2 \\ \lambda_{po} + \epsilon_p \delta \lambda_p \left(1 - \left(\frac{t''}{T_3} - \frac{1}{2\pi} \sin\left(\frac{2t''\pi}{T_3}\right) \right) \right) & , 0 \leq t'' \leq T_3 \end{cases} \quad (\text{A.4})$$

$$\mu_p(t) = \begin{cases} \mu_{po} + \epsilon_p \delta \mu_p \left(\frac{t}{T_1} - \frac{1}{2\pi} \sin\left(\frac{2t\pi}{T_1}\right) \right) & , 0 \leq t \leq T_1 \\ \mu_{po} + \epsilon_p \delta \mu_p \left(1 + 2 \left(\frac{t'}{T_2} - \frac{1}{4\pi} \sin\left(\frac{4t'\pi}{T_2}\right) \right) \right) & , 0 \leq t' \leq T_2 \\ \mu_{po} - \epsilon_p \delta \mu_p \left(\frac{t''}{T_3} - \frac{1}{2\pi} \sin\left(\frac{2t''\pi}{T_3}\right) \right) & , 0 \leq t'' \leq T_3 \end{cases} \quad (\text{A.5})$$

$$\nu_p(t) = \begin{cases} \nu_{po} + \epsilon_p \delta \nu_p \left(\frac{t}{T_1} - \frac{1}{4\pi} \sin\left(\frac{4t\pi}{T_1}\right) \right) & , 0 \leq t \leq \frac{T_1}{2} \\ \nu_{po} - \epsilon_p \left(\frac{\delta \nu_p}{2} \right) \left(1 - 4 \left(\frac{t}{T_1} - \frac{1}{4\pi} \sin\left(\frac{4t\pi}{T_1}\right) \right) \right) & , \frac{T_1}{2} \leq t \leq T_1 \\ \nu_{po} - \epsilon_p (\delta \nu_p) \left(2 \left(\frac{t'}{T_2} - \frac{1}{4\pi} \sin\left(\frac{4t'\pi}{T_2}\right) \right) \right) & , 0 \leq t' \leq \frac{T_2}{2} \end{cases} \quad (\text{A.6})$$

$$\nu_p(t) = \begin{cases} \nu_{po} + \epsilon_p \delta \nu_p \left(2 \left(1 - \frac{t'}{T_2} - \frac{1}{4\pi} \sin\left(\frac{4t'\pi}{T_2}\right) \right) \right) & , \frac{T_2}{2} \leq t' \leq T_2 \\ \nu_{po} + \epsilon_p \delta \nu_p \left(2 \left(\frac{t''}{T_2} - \frac{1}{4\pi} \sin\left(\frac{4t''\pi}{T_2}\right) \right) \right) & , 0 \leq t'' \leq \frac{T_2}{2} \\ \nu_{po} - \epsilon_p \delta \nu_p \left(1 - \left(\frac{t''}{T_3} - \frac{1}{4\pi} \sin\left(\frac{4t''\pi}{T_3}\right) \right) \right) & , \frac{T_3}{2} \leq t'' \leq T_3 \end{cases} \quad (\text{A.7})$$

Motion of the free foot

The expressions on (A.8) and (A.10) determine, within the frame $x_M - y_M - z_M$, the position of the origin O_{12} of the frame 12 on the free foot (Fig. 2). This point is ubicated on the left ankle if the right foot is on the floor, and viceversa. The orientation of the free foot is determined in relation to the frame $x_M - y_M - z_M$ and is given by the functions (A.11) and (A.13). In the Eq. (A.8) $j = 1, \dots, n_p$.

$$x_f(t) = j \delta x_f + \delta x_f \left[\frac{t}{T_{Si}} - \frac{1}{2\pi} \sin\left(\frac{2t\pi}{T_{Si}}\right) \right] \quad (\text{A.8})$$

$$y_f(t) = \begin{cases} \delta y_f (\sin(\pi x_f(t))) & , 0 \leq t \leq T_1 \\ \delta y_f \left(\sin\left(\frac{\pi}{2} \left(1 + \frac{x_f(t')}{S_x} \right) \right) \right) & , 0 \leq t' \leq T_2 \\ \delta y_f (\sin(\pi x_f(t''))) & , 0 \leq t'' \leq T_3 \end{cases} \quad (\text{A.9})$$

$$z_f(t) = \begin{cases} \delta z_f \left[\frac{2t}{T_{Si}} - \frac{1}{2\pi} \sin\left(\frac{4t\pi}{T_{Si}}\right) \right] & \text{if } t \leq \frac{T_{Si}}{2} \\ \delta z_f - \delta z_f \left[\frac{(2t - T_{Si})}{T_{Si}} - \frac{1}{2\pi} \sin\left(\frac{2\pi(2t - T_{Si})}{T_{Si}}\right) \right] & \text{if } t > \frac{T_{Si}}{2} \end{cases} \quad (\text{A.10})$$

$$\lambda_f(t) = \begin{cases} \lambda_{fo} + \delta \lambda_f \left[\frac{2t}{T_{Si}} - \frac{1}{2\pi} \sin\left(\frac{4t\pi}{T_{Si}}\right) \right] & \text{if } t \leq \frac{T_{Si}}{2} \\ \lambda_{fo} + \delta \lambda_f \left\{ 1 - \left[\frac{(2t - T_{Si})}{T_{Si}} - \frac{1}{2\pi} \sin\left(\frac{2\pi(2t - T_{Si})}{T_{Si}}\right) \right] \right\} & \text{if } t > \frac{T_{Si}}{2} \end{cases} \quad (\text{A.11})$$

$$\mu_f(t) = \begin{cases} \mu_{fo} + \delta \mu_f \left[\frac{2t}{T_{Si}} - \frac{1}{2\pi} \sin\left(\frac{4t\pi}{T_{Si}}\right) \right] & \text{if } t \leq \frac{T_{Si}}{2} \\ \mu_{fo} + \delta \mu_f \left\{ 1 - \left[\frac{(2t - T_{Si})}{T_{Si}} - \frac{1}{2\pi} \sin\left(\frac{2\pi(2t - T_{Si})}{T_{Si}}\right) \right] \right\} & \text{if } t > \frac{T_{Si}}{2} \end{cases} \quad (\text{A.12})$$

$$\nu_f(t) = \begin{cases} \nu_{fo} + \delta \nu_f \left[\frac{2t}{T_{Si}} - \frac{1}{2\pi} \sin\left(\frac{4t\pi}{T_{Si}}\right) \right] & \text{if } t \leq \frac{T_{Si}}{2} \\ \nu_{fo} + \delta \nu_f \left\{ 1 - \left[\frac{(2t - T_{Si})}{T_{Si}} - \frac{1}{2\pi} \sin\left(\frac{2\pi(2t - T_{Si})}{T_{Si}}\right) \right] \right\} & \text{if } t > \frac{T_{Si}}{2} \end{cases} \quad (\text{A.13})$$

Appendix B Inverse Kinematic Model of a 12 DOF Biped Robot

The inverse kinematic model equations for the feet of the humanoid robot are determined by a specific position and orientation frame of the pelvis with respect to the frame $x_M - y_M - z_M$, by an homogenous matrix equation expressed as:

$${}^M_p T^* = \begin{bmatrix} t_{p11} & t_{p12} & t_{p13} \\ t_{p21} & t_{p22} & t_{p23} \\ t_{p31} & t_{p32} & t_{p33} \end{bmatrix} \quad (\text{B.1})$$

The star in ${}^M_p T^*$ denotes that this matrix is known. The elements of ${}^M_p T^*$ are calculated from the operational coordinates defined in Eqs. (A.1)–(A.7). The first three rows and columns are determined by using the Bryant angles matrix, that is expressed as:

$${}^M_p R = \begin{bmatrix} c\mu c\nu & -c\mu s\nu & s\mu \\ s\lambda s\mu c\nu + c\lambda s\nu & -s\lambda s\mu s\nu + c\lambda c\nu & -s\lambda c\mu \\ -c\lambda s\mu c\nu + s\lambda s\nu & c\lambda s\mu s\nu + s\lambda c\nu & c\lambda c\mu \end{bmatrix} \quad (\text{B.2})$$

where the angles, corresponding to the pelvis, are defined by the function (A.4)–(A.7). At the same time, the three elements of the last row from ${}^M_p T^*$ are the Cartesian coordinates of the origin frame of the pelvis in the frame $x_M - y_M - z_M$, that are specified by the functions (A.1)–(A.3). The inverse kinematic equations for the free foot are obtained from the homogeneous matrix equation ${}^p_{12} T^*$ that defines the reference frame 12, present in the free foot, with respect from the frame of the pelvis. This matrix is the result of the product:

$${}^p_{12} T^* = {}^p_M T^* * {}^M_f T^* * {}^f_{12} T^* \quad (\text{B.3})$$

where ${}^p_M T^*$ is the inverse matrix given by (B.1). The homogeneous matrix equation ${}^f_{12} T^*$ from the Eq. (B.3) is:

$${}^f_{12} T^* = \begin{bmatrix} 0 & 0 & 1 & 0 \\ 1 & 0 & 0 & 0 \\ 0 & 1 & 0 & 0 \\ 0 & 0 & 0 & 1 \end{bmatrix} \quad (\text{B.4})$$

As show in Fig. 2, the elements of ${}^M_f T^*$ are calculated by the operational coordinates defined in Eqs. (A.8)–(A.13). The orientation of this matrix is determined by using the matrix (B.2), with the Bryant angles for the free foot. Finally, the known elements that results from the matrix ${}^p_{12} T^*$ are designated as follows:

$${}^p_{12}T^* = \begin{bmatrix} t_{f11} & t_{f12} & t_{f13} & t_{f14} \\ t_{f21} & t_{f22} & t_{f23} & t_{f24} \\ t_{f31} & t_{f32} & t_{f33} & t_{f34} \\ 0 & 0 & 0 & 1 \end{bmatrix} \quad (\text{B.5})$$

The inverse kinematic model is determined by using the Eqs. (B.1) and (B.5), the geometric parameters of the humanoid robot, and the walking parameters shown in Tables 1 and 2. Next we show the equations of the inverse kinematic model, where $\bar{d}_7 = (d_7/2)$:

- Support foot:

$$\begin{aligned} s_6 &= (t_{p23}r_6 - y_p)t_{p31} - (t_{p33}r_6 - z_p)t_{p21} - (t_{p21}t_{p32} - t_{p22}t_{p31} + t_{p31})\bar{d}_7 \\ c_6 &= (t_{p23}r_6 - y_p - \bar{d}_7)t_{p32} + z_p - t_{p33}r_6 \\ s_1 &= (t_{p31}c_6 - t_{p32}s_6)r_5 - t_{p32}\bar{d}_7 - t_{p33}r_6 + z_p \\ c_1 &= (t_{p21}c_6 - t_{p22}s_6)r_6 - t_{p22}\bar{d}_7 - t_{p23}r_6 + y_p + \bar{d}_7 \\ s_5 &= (t_{p21}s_1 - t_{p31}c_1)s_6 - (t_{p22}s_1 - t_{p32}c_1)c_6 \\ c_5 &= t_{p33}c_1 - t_{p23}s_1 \\ x_{14} &= (t_{p21}c_1c_6 + t_{p31}s_1c_6 - t_{p22}c_1s_6 - t_{p32}s_1s_6)r_5 - (t_{p22}c_1 + t_{p32}s_1)\bar{d}_7 + \\ &\quad (y_p - t_{p23}r_6 + \bar{d}_7)c_1 + (z_p - t_{p33}r_6)s_1 \\ z_{14} &= (t_{p11}c_6 - t_{p12}s_6)r_5 - t_{p12}\bar{d}_7 - t_{p13}r_6 + x_p \\ r_{14} &= \sqrt{(x_{14})^2 + (z_{14})^2} \\ r_{t\alpha x} &= \frac{x_{14}}{r_{14}}\sqrt{d_3^2 - 0.25(r_{14})^2} + 0.5z_{14} \\ r_{t\alpha y} &= \frac{x_{14}}{2} - \frac{z_{14}}{r_{14}}\sqrt{d_3^2 - 0.25(r_{14})^2} \\ r_{f\alpha x} &= z_{14} - r_{t\alpha x} \\ r_{f\alpha y} &= x_{14} - r_{t\alpha y} \\ s_{2\bar{3}4} &= -(t_{p11}s_6 + t_{p12}c_6)c_5 - t_{p13}s_5 \\ c_{2\bar{3}4} &= t_{p11}c_6 - t_{p12}s_6 \\ \theta_1 &= \text{atan2}(s_1, c_1) \\ \theta_2 &= \text{atan2}(r_{t\alpha y}, r_{t\alpha x}) - 0.5\pi \\ \theta_3 &= \text{atan2}(r_{f\alpha y}, r_{f\alpha x} - \theta_2 - 0.5\pi) \\ \theta_4 &= \text{atan2}(s_{2\bar{3}4}, c_{2\bar{3}4}) - \theta_2 - \theta_3 \\ \theta_5 &= \text{atan2}(s_5, c_5) \\ \theta_6 &= \text{atan2}(s_6, c_6) \end{aligned}$$

- Free foot:

$$\begin{aligned}
s_7 &= t_{f23}z_f + (\bar{d}_7 + y_f)t_{f23} \\
c_7 &= t_{f33}x_f - t_{f13}z_f \\
s_8 &= z_f \\
c_8 &= x_f s_7 - (\bar{d}_7 - y_f)c_7 \\
x_{812} &= (x_f s_7 + (y_f - \bar{d}_7)c_7)c_8 + z_f s_8 \\
z_{812} &= (\bar{d}_7 - y_f)s_7 + x_f c_7 - r_8 \\
r_{812} &= \sqrt{(x_{812})^2 + (z_{812})^2} \\
r_{flx} &= \frac{x_{812}}{r_{812}} \sqrt{d_{10}^2 - 0.25(r_{812})^2} + 0.5z_{812} \\
r_{fly} &= \frac{x_{812}}{2} - \frac{z_{812}}{r_{812}} \sqrt{d_{10}^2 - 0.25(r_{812})^2} \\
r_{tlx} &= z_{812} - r_{flx} \\
r_{tly} &= x_{812} - r_{fly} \\
g_{11} &= t_{g13}c_7 - t_{f23}s_7 \\
s_{12} &= t_{f31}c_8 - (t_{f11}s_7 + t_{f21}c_7)s_8 \\
c_{12} &= t_{f32}c_8 - (t_{f12}s_7 + t_{f22}c_7)s_8 \\
\theta_7 &= \text{atan2}(s_7, c_7) \\
\theta_8 &= \text{atan2}(s_8, c_8) \\
\theta_9 &= \text{atan2}(r_{fly}, r_{flx}) - 0.5\pi \\
\theta_{10} &= \text{atan2}(r_{tly}, r_{tlx}) - \theta_9 - 0.5\pi \\
c_{910} &= \cos(\theta_9 + \theta_{10}) \\
s_{910} &= \sin(\theta_9 + \theta_{10}) \\
h_{11} &= \sqrt{(s_{910})^2 + (c_{910})^2 - (g_{11})^2} \\
\theta_{11} &= \text{atan2}((-s_{910}g_{11} - c_{910}h_{11}), (c_{910}g_{11} - s_{910}h_{11})) \\
\theta_{12} &= \text{atan2}(s_{12}, c_{12})
\end{aligned}$$

References

1. Kato, I.: Development of WABOT 1. *Biomechanism*, **2**, 173–214 (1973)
2. Kornblum, J.: Meet Hondas ASIMO, a helpful Mr. Roboto. USA-Today (2000)
3. Honda unveils all-new ASIMO with significant advancements. <http://hondanews.com/releases/cd29e4c7-c889-4378-a86a-3534ed615459>. Accessed 30 Sep 2016
4. Kaneko, K., Kanehiro, F., Morisawa, M., Miura, K., Nakaoka, S., Kajita, S.: Cybernetic human HRP-4C. In: 9th IEEE-RAS International Conference on Humanoid Robots, pp. 7–14. IEEE (2009)
5. Diftler, M., Mehling, J., Abdallah, M., Radford, N., Bridgwater, L., Sanders, A., Askew, R., Linn, D., Yamokoski, J., Permenter, F., et al.: Robonaut 2-the first humanoid robot in space. In: IEEE International Conference on Robotics and Automation (ICRA), pp. 2178–2183. IEEE (2011)

6. Aldebaran robotics announces NAO Next Gen humanoid robot. <https://www.engadget.com/2011/12/10/aldebaran-robotics-announces-nao-next-gen-humanoid-robot-video/>. Accessed 30 Sep 2016
7. Chestnutt, J., Lau, M., Cheung, G., Kuffner, J., Hodgins, J., Kanade, T.: Footstep planning for the Honda ASIMO humanoid. In: Proceedings of the IEEE International Conference on Robotics and Automation, pp. 629–634. IEEE (2005)
8. Jiwen, Z., Li, L., Ken, C.: Footstep planning for rapid path following in humanoid robots. *Int. J. Humanoid Rob.* **13**(4), 1650013 (2016)
9. Sakamoto, H., Katayose, H., Miyazaki, K., Nakatsu, R.: Extended-knee walk for humanoid robot with parallel link legs. *Int. J. Humanoid Rob.* **6**(04), 565–584 (2009)
10. Castano, J., Li, Z., Zhou, C., Tsagarakis, N., Caldwell, D.: Dynamic and reactive walking for humanoid robots based on foot placement control. *Int. J. Humanoid Rob.* **13**(02), 1550041 (2016)
11. Omran, S., Sakka, S., Aoustin, Y.: Effects of the COM vertical oscillation on joint torques during 3d walking of humanoids robots. *Int. J. Humanoid Rob.* **13**(4), 1650019 (2016)
12. Yang, L., Liu, Z., Zhang, Y.: Online walking control system for biped robot with optimized learning mechanism: an experimental study. *Nonlinear Dyn.* **86**(3), 2035–2047 (2016)
13. Strom, J., Slavov, G., Chown, E.: Omnidirectional walking using ZMP and preview control for the NAO humanoid robot. In: Baltes, J., Lagoudakis, M.G., Naruse, T., Ghidary, S.S. (eds.) *RoboCup 2009. LNCS (LNAI)*, vol. 5949, pp. 378–389. Springer, Heidelberg (2010). doi:[10.1007/978-3-642-11876-0_33](https://doi.org/10.1007/978-3-642-11876-0_33)
14. Dong, E., Wang, D., Chen, C., Tong, J.: Realization of biped robot gait planning based on NAO robot development platform. In: IEEE International Conference on Mechatronics and Automation (ICMA), pp. 1073–1077. IEEE (2016)
15. Liu, J., Urbann, O.: Bipedal walking with dynamic balance that involves three-dimensional upper body motion. *Rob. Auton. Syst.* **77**, 39–54 (2016)
16. Hashemi, E., Khajepour, A.: Kinematic and three-dimensional dynamic modeling of a biped robot. *Proc. Inst. Mech. Eng. Part K J. Multi-body Dyn.* 1464419316645243 (2016)
17. Khalil, W., Kleinfinger, J.: A new geometric notation for open and closed-loop robots. In: IEEE International Conference on Robotics and Automation, Proceedings, vol. 3, pp. 1174–1179. IEEE (1986)
18. Pamanes, J.A.: Modelado cinemático del robot humanoide bioloid. Technical report, Facultad de la ingeniería mecánica y eléctrica de la Universidad Autónoma de Coahuila (2009)
19. Fierro, J., Pamanes, J.A., Santibanez, V., Ruiz, G., Ollervides, J.: Condiciones para una marcha elemental del robot NAO. *AMRob J. Rob. Theor. Appl.* **4**(1), 13–18 (2014)
20. Arias, L., Olvera, L., Pamanes, J.A., Nunez, J.: Patrón de marcha 3d de tipo cicloidal para humanoides y su aplicación al robot bioloid. *Revista Iberoamericana de Ingeniería Mecánica* **18**, 03–22 (2014)

Advances in Automation and Robotics Research in Latin America

Proceedings of the 1st Latin American Congress on Automation and Robotics, Panama City, Panama 2017
Chang, I.; Baca, J.; Moreno, H.A.; Carrera, I.G.; Cardona, M.N. (Eds.)

2017, IX, 310 p. 205 illus., Softcover

ISBN: 978-3-319-54376-5